

## Synthesis and properties of single-crystal $\beta_3$ -Ni<sub>3</sub>Si nanowires

Yipu Song and Song Jin<sup>a)</sup>

Department of Chemistry, University of Wisconsin-Madison, Madison, Wisconsin 53706

(Received 7 March 2007; accepted 30 March 2007; published online 26 April 2007)

Single-crystal Ni<sub>3</sub>Si nanowires were synthesized by a chemical vapor transport method, using iodine as the transport reagent. Structural characterization using powder x-ray diffraction, electron microscopy, and energy dispersive spectroscopy confirms that the nanowires are the monoclinic  $\beta_3$ -Ni<sub>3</sub>Si phase. Four-terminal electrical measurements show that the single-crystal nanowires have a resistivity of 72  $\mu\Omega$  cm and are capable of supporting a high failure current density about  $1.7 \times 10^7$  A/cm<sup>2</sup>. These unique Ni<sub>3</sub>Si nanowires are attractive nanoscale building blocks for interconnects and for fully silicided gate application in nanoelectronics. © 2007 American Institute of Physics. [DOI: 10.1063/1.2732828]

Transition metal silicides are very important to complementary metal-oxide-semiconductor (CMOS) transistors as Ohmic contact and interconnect, and more recently gate.<sup>1,2</sup> Among them, nickel silicides have recently attracted attention as choice fully silicided (FUSI) metal gates to replace the current polysilicon gates in the future 45 nm CMOS device node due to absent polydepletion effects, low resistance, and suitably tunable work functions.<sup>3</sup> Owing to the unique range of properties, such as high melting point and excellent thermal stability, the metal-rich silicide Ni<sub>3</sub>Si has been identified as a highly promising candidate for a diverse field of applications.<sup>4</sup> Additionally, Ni<sub>3</sub>Si and Ni<sub>2</sub>Si are the most suitable materials for *p*-MOS applications based on their work functions ( $\sim 4.8$  eV) and there has already been demonstration employing Ni<sub>3</sub>Si as the FUSI metal gate in *p*-MOS devices.<sup>5</sup> An approach to nanoelectronics is the bottom-up assembly of one-dimensional (1D) nanowires (NWs) with cross nanowire assembly for functional nanosystems.<sup>6,7</sup>

Freestanding Ni<sub>3</sub>Si nanowires have not yet been reported. It has been previously reported that NiSi and Ni<sub>2</sub>Si nanowires were formed by decomposing silane gas<sup>8</sup> or sputtering silicon<sup>9</sup> onto Ni surfaces, and by other synthesis strategies.<sup>10,11</sup> Silicides are usually refractory materials with high melting points. Simply heating the silicide solid is often not effective in delivering the materials with sufficient vapor pressures necessary for vapor phase nanowire syntheses. We have developed a chemical vapor transport (CVT) method to prepare Ni<sub>2</sub>Si NWs using iodine (I<sub>2</sub>) as the chemical transport reagent and Ni<sub>2</sub>Si powder as source material.<sup>12</sup> This CVT approach can be generally applicable for the vapor phase synthesis of other refractory materials and complements the more controllable CVD synthesis of silicide NWs using single source precursors.<sup>13</sup> In this letter, we report a direct chemical synthesis of single-crystal  $\beta_3$ -Ni<sub>3</sub>Si NWs using CVT delivery of TiSi<sub>2</sub> powder, which has higher melting point (1760 °C) than nickel silicides, in combination with application of nickel nitrate [Ni(NO<sub>3</sub>)<sub>2</sub>] salt on substrates. The resulting Ni<sub>3</sub>Si NWs were structurally characterized and found to have good resistivity and failure current densities

making them attractive for nanoelectronic gate and interconnect applications.

All NW syntheses were performed in a home-built continuous flow chemical vapor transport (CVT) reactor which is comprised of a sealed 1 in. quartz tube heated by a single-zone split tube furnace (Lindberg/Blue M). Iodine powder (2 g) in an alumina boat was placed in the quartz tube upstream just outside of the tube furnace and TiSi<sub>2</sub> powder (from Aldrich, 500 mg, usually 10–20 mg was consumed) in an alumina boat was placed in the center of the tube furnace. At high temperatures ( $T_1=970$  °C) sublimed iodine reacts with silicide to produce gaseous products of metal iodide and silicon iodide that are carried downstream by argon gas flow to a different temperature zone ( $T_2 \approx 830$  °C) where the thermodynamics of the reaction reverses favorability. Si/SiO<sub>2</sub> substrates, on which several drops of aqueous Ni(NO<sub>3</sub>)<sub>2</sub> solution (0.1M) have been dispersed and air dried, were placed downstream in this heating zone. For typical reactions, the tube reactor was flushed with argon at 20 SCCM (SCCM denotes cubic centimeter per minute at STP) for 30 min, and then heated to 970 °C (temperature at the center) for 4–5 h under argon flow (20 SCCM) at atmospheric pressure. The morphology of the as grown products was examined using a field emission scanning electron microscope (SEM, LEO SUPRA 1530). Large amount of entangled freestanding Ni<sub>3</sub>Si NWs are found in the dark gray regions on the substrates. Representative SEM image [Fig. 1(a)] from the gray layers on the substrate revealed straight and long NWs having 40–80 nm diameters and 10  $\mu$ m length in high yield. Bundles of NWs can also be seen from the dark gray areas on the substrate, as shown in the Fig. 1(b). The best NW growth in terms of morphology and yield was observed for substrates located in the temperature range of 810–850 °C.

The product was also characterized using powder x-ray diffraction (PXRD), as shown in Fig. 2. All major diffraction peaks can be matched to that of the monoclinic  $\beta_3$  phase of Ni<sub>3</sub>Si (Person symbol *mC*16).<sup>14</sup> The calculated lattice parameters from PXRD data:  $a=7.04$  Å,  $b=6.26$  Å,  $c=5.08$  Å, and  $\beta=131.2^\circ$  are in good agreement with the literature.<sup>14</sup> No other nickel silicide phases or other crystalline impurity phases, such as those containing titanium, are detectable by PXRD.

The chemical composition of the nanowires was analyzed by energy dispersive spectroscopy (EDS) [Fig. 3(a)],

<sup>a)</sup> Author to whom correspondence should be addressed; electronic mail: jin@chem.wisc.edu

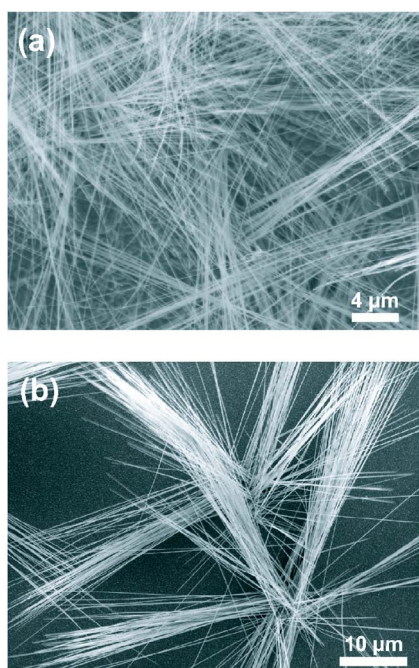


FIG. 1. (Color online) Representative SEM images of (a) as grown  $\text{Ni}_3\text{Si}$  nanowires from the dense gray layers and (b) NW bundles from the dark gray areas on the growth substrate.

which reveals that the NWs consist of only Ni, Si, and trace amounts of O elements. Importantly, Ti element was never detected from either single NWs or NW bundles. The atomic ratio of Ni:Si is about 17:8, which deviates from the chemical stoichiometry ratio for  $\text{Ni}_3\text{Si}$ . This could be partially accounted for by the thin silicon oxide layer on the nanowire surface. These NWs were further characterized using transmission electron microscopy (TEM, Philips CM200). A representative low-magnification TEM image of typical NWs is shown in Fig. 3(b). All selected area electron diffraction (SAED) patterns recorded from single NWs [inset of Fig. 3(b)] reveal the single-crystalline structure of the NWs and can be indexed to the monoclinic  $\beta_3\text{-Ni}_3\text{Si}$  structure along the  $[00\bar{1}]$  zone axis. A representative high-resolution TEM (HRTEM) image [Fig. 3(c)] of a  $\text{Ni}_3\text{Si}$  NW clearly shows lattice fringes of a single-crystal NW and an oxide layer about 8 nm thick on the surface. The measured lattice spacings observed in HRTEM are 1.98 Å, which correspond well to the  $(\bar{2}22)$  lattice spacings of the  $\beta_3\text{-Ni}_3\text{Si}$  structure. The two-dimensional fast Fourier transform (FFT) of the lattice resolved image [inset of Fig. 3(c)] shows the reciprocal lat-

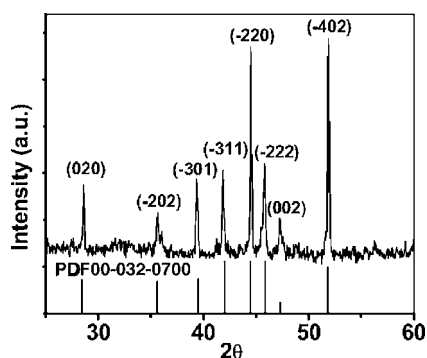


FIG. 2. Powder x-ray diffraction pattern from as grown sample of  $\text{Ni}_3\text{Si}$  nanowires.

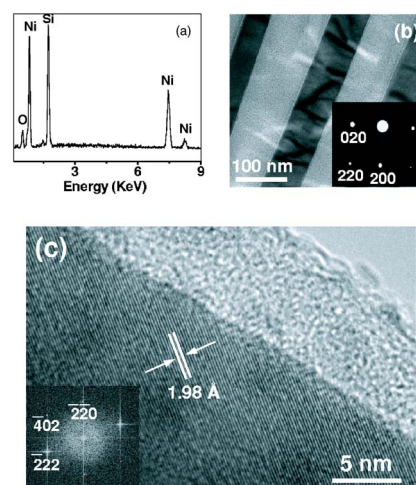


FIG. 3. (Color online) (a) EDS spectrum of the typical NW. (b) Representative low-magnification TEM image of  $\text{Ni}_3\text{Si}$  NWs. The inset shows the SAED pattern of the NW along the  $[00\bar{1}]$  zone axis. (c) Representative HRTEM image of a  $\text{Ni}_3\text{Si}$  NW and the corresponding indexed two-dimensional FFT (inset).

tice peaks, which can be indexed to a  $C$ -centered monoclinic lattice.

In typical CVT reactions, the transport reagent iodine reacts with about 10–20 mg  $\text{TiSi}_2$  powder at high temperatures and the resulting precursors are delivered to supply the silicon for NW growth at lower temperature. This CVT process is essential to NW growth as no products were observed on the substrates if either the transport reagent iodine or the source material  $\text{TiSi}_2$  were not used in the reactions under otherwise identical conditions. However, Ti is not observed in the NW products based on the structural and chemical analyses above. The gaseous  $\text{TiI}_4$  must have been flushed out of the flow reactor or reacted with trace amount of oxygen along the way. The presence of  $\text{Ni}(\text{NO}_3)_2$  is obviously crucial to the formation of  $\text{Ni}_3\text{Si}$  NWs because that is the source of Ni. It is likely that Ni [from  $\text{Ni}(\text{NO}_3)_2$ ] can simultaneously provide the initial nucleation sites for the incoming silicon iodide gas and serve as the Ni feedstock for NW growth. Such metal-assisted NW growth has often been observed before.<sup>6,7</sup> The fact that nickel silicide is formed as the product instead of  $\text{TiSi}_2$  may come from several factors. Titanium silicides have higher eutectic temperatures compared with nickel silicides and previous CVT growth of  $\text{TiSi}_2$  single crystals has always been performed in *sealed tubes* where a saturation in  $\text{TiI}_4$  vapor would force Ti reaction/deposition.<sup>15</sup> Our CVT reactions, in contrast, are performed in an *open* continuous flow system, where there is no guarantee that equilibrium is reached in the different temperature zones. It was also found that  $\text{Cl}_2$  was a much better (faster) transport agent for CVT of  $\text{TiSi}_2$  than either  $\text{Br}_2$  or  $\text{I}_2$ . This slow delivery is likely the reason that the NW product is the most nickel-rich silicide phase.

To investigate the electrical properties of these single-crystal  $\text{Ni}_3\text{Si}$  NWs, we fabricated four-terminal NW devices using a standard e-beam lithography technique. Prior to evaporating Ti/Au metal leads, the NWs are etched in buffer HF solution for 10 s to remove the oxide layer, rinsed in de-ionized water for 10 s, and dried in a nitrogen flow. For  $\text{Ni}_3\text{Si}$  NW devices, the current ( $I$ ) versus voltage ( $V$ ) curves display a perfect linear  $I$ - $V$  behavior, as shown for a repre-

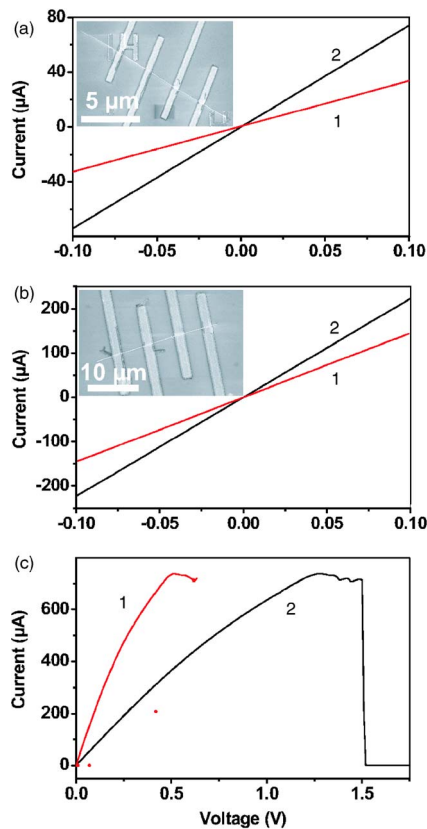


FIG. 4. (Color online) Transport measurements on Ni<sub>3</sub>Si nanowires. [(a) and (b)] Current vs voltage curves recorded for two Ni<sub>3</sub>Si nanowires with a diameter of (a) 56 nm and (b) 76 nm, with red line (1) and black line (2) corresponding to two- and four-terminal measurements, respectively. (insets) SEM image of the devices measured. (c) Current vs voltage recorded for the Ni<sub>3</sub>Si NW device shown in (b) that breaks down at higher voltage and current, with red line (1) and black line (2) corresponding to four-terminal measurement and two-outermost-contact measurement, respectively.

sentative device in Fig. 4(a). Four-terminal  $I$ - $V$  measurements were conducted by driving a known current between the two outermost contacts while the potential difference was measured between the two inner contacts [Fig. 4(a) inset]. Two- (red line 1) and four-terminal (black line 2)  $I$ - $V$  measurements yield resistance of 2.94 k $\Omega$  and 1.35 k $\Omega$ , respectively, for this 4.7  $\mu\text{m}$  long Ni<sub>3</sub>Si NW device with a diameter of  $56 \pm 1$  nm, which corresponds to a resistivity of  $153 \pm 2$  and  $71 \pm 1$   $\mu\Omega$  cm for two- and four-terminal measurements, respectively. Measurements of five devices gave an average four-terminal resistivity of  $72 \pm 1$   $\mu\Omega$  cm for Ni<sub>3</sub>Si NWs. This resistivity value is lower than that reported for polycrystalline Ni<sub>3</sub>Si (82  $\mu\Omega$  cm),<sup>16</sup> which can be attributed to the single-crystal structure in our case. Although the resistivity of Ni<sub>3</sub>Si is higher than that of NiSi and Ni<sub>2</sub>Si, it is still much lower than state of the art polysilicon gate materials.<sup>16</sup>

The maximum transport current density ( $J_{\text{max}}$ ) was also characterized for the Ni<sub>3</sub>Si NWs using four-terminal measurements. A NW device [inset of Fig. 4(b)] with a two- and four-terminal resistivity of  $114 \pm 2$  and  $73 \pm 1$   $\mu\Omega$  cm, respectively [Fig. 4(b)] was used for the breakdown test. Figure 4(c) shows the breakdown test for this NW device: black line 2 is the measurement between the two outermost contacts and red line 1 is the four-terminal measurement. The break-

down test is typical with the NW displaying a maximum current of 0.741 mA before a precipitous drop to zero, corresponding to a high failure current density ( $J_{\text{max}}$ ) of about  $1.7 \times 10^7$  A/cm<sup>2</sup>. Breakdown tests for more devices show that the NWs usually break down at a current level of 0.4–0.8 mA when voltages are above 0.5 V for four-terminal measurement or 1.2 V for two-outermost-contact measurement. The maximum current densities ( $J_{\text{max}}$ ) are always greater than  $1 \times 10^7$  A/cm<sup>2</sup>. Ni<sub>3</sub>Si NWs have good resistivity and reasonably high failure current densities making them attractive 1D nanoscale building blocks for interconnect and gates in nanoelectronic devices. In bottom-up assembled nanoelectronic circuits built with cross nanowire arrays, these metallic Ni<sub>3</sub>Si NWs could serve as “fully silicided” gates with suitable work function for cross nanowire<sup>17</sup> FET devices<sup>6,7</sup> having gate lengths as small as the nanowire cross points.

In summary, Ni<sub>3</sub>Si nanowires were synthesized by a chemical vapor transport (CVT) method, using iodine as the transport reagent. Structural characterization shows that the nanowires are single crystals with monoclinic  $\beta$ -Ni<sub>3</sub>Si structure, even though TiSi<sub>2</sub> was used as the source material. Electrical measurements show that these nanowires have an average resistivity of 72  $\mu\Omega$  cm and are capable of supporting high failure current density of about  $1.7 \times 10^7$  A/cm<sup>2</sup>. These unique Ni<sub>3</sub>Si nanowires are attractive nanoscale building blocks for interconnects and fully silicided (FUSI) gate application in nanoelectronics.

This research is supported by a WARF Draper TIF grant. One of the authors (S.J.) thanks NSF (CAREER DMR-0548232), 3M Nontenured Faculty Award, and DuPont S&E grant for financial support. The authors thank Andrew L. Schmitt for the critical reading of the manuscript.

- <sup>1</sup>M. Leong, V. Narayanan, D. Singh, A. Topol, V. Chan, and Z. Ren, *Mater. Today* **9**, 26 (2006).
- <sup>2</sup>S. L. Zhang and M. Ostling, *Crit. Rev. Solid State Mater. Sci.* **28**, 1 (2003).
- <sup>3</sup>J. A. Kittl, A. Lauwers, M. A. Pawlak, M. J. H. vanDal, A. Veloso, K. G. Anil, G. Pourtois, C. Demeurisse, T. Schram, B. Brijs, M. dePotter, C. Vrancken, and K. Maex, *Microelectron. Eng.* **82**, 441 (2005).
- <sup>4</sup>A. T. Dutra, P. L. Ferrandini, C. A. R. Costa, M. C. Goncalves, and R. Caram, *J. Alloys Compd.* **399**, 202 (2005).
- <sup>5</sup>J. A. Kittl, M. A. Pawlak, A. Lauwers, C. Demeurisse, K. Opsomer, K. G. Anil, C. Vrancken, M. J. H. vanDal, A. Veloso, S. Kubicek, P. Absil, K. Maex, and S. Biesemans, *IEEE Electron Device Lett.* **27**, 34 (2006).
- <sup>6</sup>Y. Xia, P. Yang, Y. Sun, Y. Wu, B. Mayers, B. Gates, Y. Yin, F. Kim, and H. Yan, *Adv. Mater. (Weinheim, Ger.)* **15**, 353 (2003).
- <sup>7</sup>Y. Li, F. Qian, J. Xiang, and C. M. Lieber, *Mater. Today* **9**, 18 (2006).
- <sup>8</sup>X. Q. Yan, H. J. Yuan, J. X. Wang, D. F. Liu, Z. P. Zhou, Y. Gao, L. Song, L. F. Liu, W. Y. Zhou, G. Wang, and S. S. Xie, *Appl. Phys. A: Mater. Sci. Process.* **79**, 1853 (2004).
- <sup>9</sup>J. Kim and W. A. Anderson, *Nano Lett.* **6**, 1356 (2006).
- <sup>10</sup>Y. Wu, J. Xiang, C. Yang, W. Lu, and C. M. Lieber, *Nature (London)* **430**, 61 (2004).
- <sup>11</sup>Z. Zhang, P. E. Hellstrom, M. Ostling, S. L. Zhang, and J. Lu, *Appl. Phys. Lett.* **88**, 043104 (2006).
- <sup>12</sup>Y. Song, A. L. Schmitt, and S. Jin, *Nano Lett.* **7**, 965 (2007).
- <sup>13</sup>A. L. Schmitt, M. J. Bierman, D. Schmeisser, F. J. Himpfel, and S. Jin, *Nano Lett.* **6**, 1617 (2006).
- <sup>14</sup>P. Ram and S. Bhan, *Z. Metallkd.* **66**, 521 (1975).
- <sup>15</sup>P. Peshev and M. Khristov, *J. Less-Common Met.* **117**, 361 (1986).
- <sup>16</sup>T. Iijima, A. Nishiyama, Y. Ushiku, T. Ohguro, I. Kunishima, K. Suguro, and H. Iwai, *IEEE Trans. Electron Devices* **40**, 371 (1993).
- <sup>17</sup>D. Whang, S. Jin, Y. Wu, and C. M. Lieber, *Nano Lett.* **3**, 1255 (2003).